

Original Article

Stability of preclinical models of aggressive renal cell carcinomas

Mariana Varna^{1,2,3*}, Guilhem Bousquet^{1,2,3*}, Irmene Ferreira^{1,2,3}, Marie Goulard^{1,2}, Morad El-Bouchtaoui^{1,2,3}, Pierre Mongiat Artus^{1,2,5}, Jérôme Verine^{1,2,3}, Eric de Kerviler^{1,2,6}, Lucie Hernandez¹, Christophe Leboeuf^{1,2,3}, Bernard Escudier⁷, Luc Legrès^{1,2}, Niclas Setterblad⁴, Hany Soliman⁴, Jean-Paul Feugeas⁴, Anne Janin^{1,2,3*}, Philippe Bertheau^{1,2,3*}

¹Université Paris Diderot, Sorbonne Paris Cité, F-75010 Paris, France; ²INSERM, U1165, Paris, F-75010 France; ³AP-HP-Hôpital Saint-Louis, Laboratoire de Pathologie, Paris, F-75010 France; ⁴AP-HP-Hôpital Saint-Louis, Service de Biochimie, Paris, F-75010 France; ⁵AP-HP-Hôpital Saint-Louis, Service d'Urologie, Paris, F-75010 France; ⁶AP-HP-Hôpital Saint-Louis, Service de Radiologie, Paris, F-75010 France; ⁷Institut Gustave Roussy, Villejuif, F-94805 France. *Equal contributors.

Received March 31, 2014; Accepted May 25, 2014; Epub May 15, 2014; Published June 1, 2014

Abstract: Renal-cell carcinomas (RCC) are often resistant to conventional cytotoxic agents. Xenograft models are used for *in vivo* preclinical studies and drug development. The validity of these studies is highly dependent on the phenotypic and genotypic stability of the models. Here we assessed the stability of six aggressive human RCC xenografted in nude/NMRI mice. We compared the initial samples (P0), first (P1) and fifth (P5) passages for the following criteria: histopathology, immunohistochemistry for CK7, CD10, vimentin and p53, DNA allelic profiles using 10 microsatellites and CGH-array. Next we evaluated the response to sunitinib in primary RCC and corresponding xenografted RCC. We observed a good overall stability between primary RCC and corresponding xenografted RCC at P1 and P5 regarding histopathology and immunohistochemistry except for cytokeratin 7 (one case) and p53 (one case) expression. Out of 44 groups with fully available microsatellite data (at P0, P1 and P5), 66% (29 groups) showed no difference from P0 to P5 while 34% (15 groups) showed new or lost alleles. Using CGH-array, overall genomic alterations at P5 were not different from those of initial RCC. The xenografted RCC had identical response to sunitinib therapy compared to the initial human RCC from which they derive. These xenograft models of aggressive human RCC are clinically relevant, showing a good histological and molecular stability and are suitable for studies of basic biology and response to therapy.

Keywords: Xenograft, preclinical model, renal cell carcinoma, tumor phenotype, tumor genotype

Introduction

Renal cell carcinomas (RCC) are hypervascularized tumors with high metastatic potential. They are often resistant to conventional cytotoxic agents [1, 2]. Therapies targeting angiogenesis have improved the prognosis of patients with metastatic RCC [3]. However, secondary resistance to this treatment is often observed [4, 5]. For this reason, development of animal models based on xenografts of the different types of RCC is essential to test new therapies via sequential analyses. Strategies to obtain these models are injection of established human tumor cell lines or direct implan-

tation of primary human cancer samples into immunodeficient nude or SCID mice [6-9].

The relevance of xenografted models depends on their similarity to the histological, biochemical and metastatic patterns observed in the initial human cancer [6, 10, 11]. Human cancer xenografts can be useful preclinical models to study response to chemotherapy [12-14]. However, in some studies, xenograft models inconsistently predicted the efficiency of novel therapies in selected human tumors [15]. For these reasons a validation of phenotypic and genotypic stability of xenografted models is an important prerequisite for the use of these models in preclinical studies.

Renal cancer xenografts stability

Table 1. Histopathological and immunohistochemical characteristics (CK7, CD10, Vimentin, p53) of six renal tumors in patients (P0) and in xenografts at 5th passage (P5)

tumor ID	age of patient (years)	sex	tissue sample	H&E	Fuhrman nuclear grade		TNM	metastasis	CK7		CD10		Vimentin		p53	
				P0	P0	P5			P0	P5	P0	P5	P0	P5	P0	P5
K6-194	60	M	B	pRCC	4	4	pT3bNxM1	bone	neg	neg	pos	pos	80%	80%	N15%	N15%
K8-128	73	M	SS	ccRCC	2	2	pT1aNxM1	lung	10%	20%	pos	pos	90%	90%	neg	C 95%
K8-447	68	M	SS	ccRCC	4	4	pT4NxM1	lung	neg	10%	pos	pos	neg	neg	neg	neg
K8-614	57	M	SS	ccRCC/src	4	4	pT3aNxM1	lung, liver	neg	60%	60%	60%	80%	80%	neg	neg
K9-162	64	M	SS	ccRCC	3	3	pT1aN0M1	bone	neg	neg	neg	neg	neg	neg	neg	neg
K9-229	63	M	B	ccRCC	4	4	pT3NxM1	lung, liver	50%	50%	60%	60%	90%	90%	C 50% N10%	C 50% N10%

ccRCC: clear-cell renal-cell carcinoma; pRCC: papillary renal-cell carcinoma; src: sarcomatoid; B: biopsy; SS: surgical specimen; C: cytoplasmic staining; N: nuclear staining.

Table 2. Microsatellite markers used for characterisation of initial human tumors and their xenografts

Microsatellite marker	Locus	% heterozygosity	Size (base pair)	Gene
D3S1289	3p14.3	81	235-253	VHL
D3S1597	3p25.3	80	162-180	VHL
D3S3611	3p25.3	82	107-137	VHL
D5S2095	5p15.31	89	141-183	Semaphorin5A
D6S440	6q25.1	67	269-285	ESR1
D8S1820	8p21.1	74	103-117	Elongation protein 3
D9S162	9p22.1	74	172-196	SLC24A2
D9S171	9p21.3	80	159-177	MLLT3
D17S802	17q25.3	82	166-183	BIRC5
D17S1879	17p13.1	82	141-173	P53 intron

We established a panel of six human RCC xenografts in nude mice and we evaluated the phenotypic and genotypic stability of these models. Immunohistochemical markers known to be frequently expressed in RCC (CD10, CK7, vimentin) or involved in oncogenesis (p53) were tested at P0, P1 and P5. DNA microsatellite profiles and CGH-array were performed at different passages. To validate these preclinical models we compared the response to an anti-angiogenic treatment (sunitinib) in tumor xenograft and in the initial tumor.

Materials and methods

Patients and tissue samples

Fresh samples were obtained from 40 human renal tumors between 2006 and 2009. A piece of tumor tissue was immediately transported in RPMI-1640 to the Animal facility for xenografting into nude mice. Informed consent was obtained from each patient. The study was approved by the University Board Ethics Committee, and conducted in accordance with the Declaration of Helsinki. Other tumor sam-

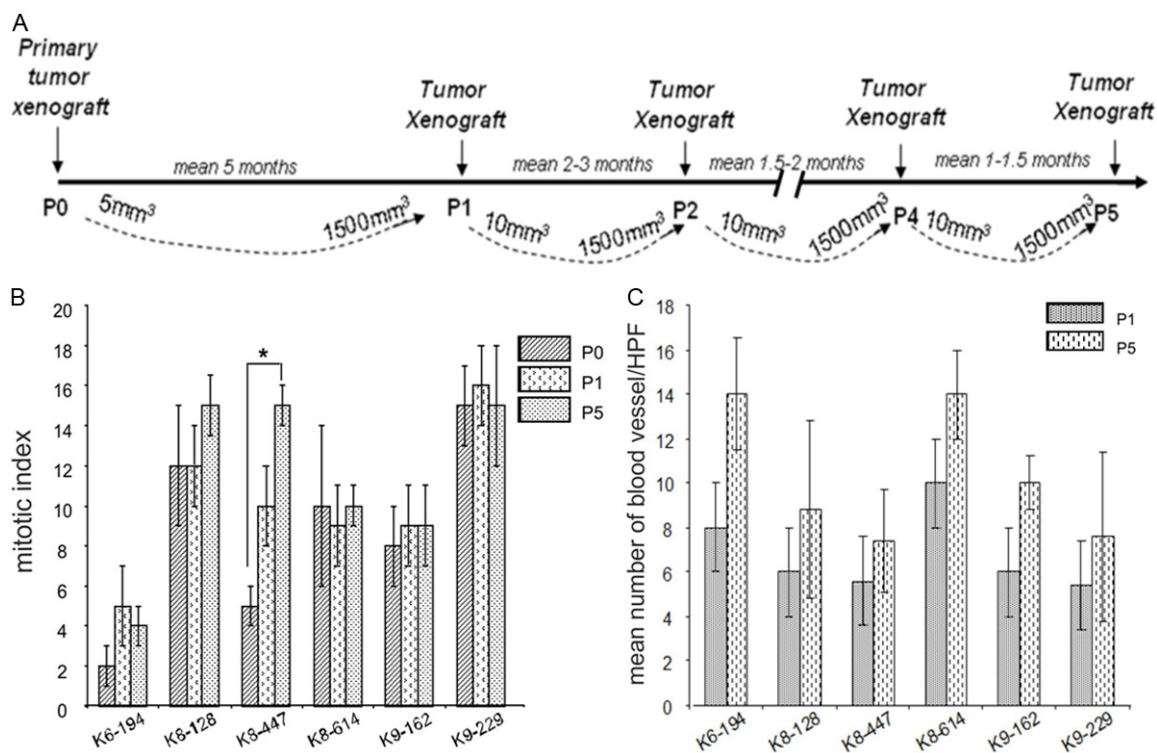


Figure 1. Tumor xenograft procedure. Time lapse for primary tumor xenograft and the subsequent passages (A); Mitotic index (B) and mean number of blood vessels for initial tumor and tumor xenografts (C); * $P < 0.001$.

ples were provided by Tumorotheque of Saint Louis Hospital (Paris, France), following the national ethics and legal French rules for patient information and consent. Histopathological features of the 6 RCC that achieved successful xenograft are described in **Table 1**.

For patients with metastatic renal cell carcinoma treated with sunitinib, tumor response was assessed every three months on computed tomography according to modified RECIST (response valuation criteria in solid tumors) criteria [16], and the best response was considered, *i.e.* complete response, partial response, stable disease or progression disease.

Xenografts of human RCC

Females, aged five to eight weeks, nu/nu athymic mice of NMRI (R. Janvier, France) background were used as xenograft recipients for human kidney tumors. The mice were bred in the Animal facility, University Institute of Haematology, Paris, France. All the mouse experiments reported in this study were approved by the Animal Housing and Experiment Board of the French government.

For the initial xenograft, 5 mm³ human tumor fragments were grafted sub-cutaneously in 5 to 10 mice under xylasin (10 mg/kg body weight) and ketamin anaesthesia (100 mg/kg body weight). For each further passage, 10 mm³ fragments were xenografted into five mice.

A clinical score was assessed daily and tumor growth measured in two perpendicular diameters with a calliper. Tumor volume was calculated as $V = L \times l^2/2$, L being the largest diameter (length), l the smallest (width) [13, 17]. Mice were euthanized when the tumors approached 1500 mm³.

For each mouse, the tumors, as well as the different organs, were systematically analysed. Tumors were dissected and cut into three parts: one part was immediately snap-frozen in liquid nitrogen, one part was formalin-fixed and paraffin-embedded, and a third part was used for the new passage.

Experimental sunitinib treatment

Three xenografted tumors K6-194, K8-614 and K9-162, were treated with sunitinib. When

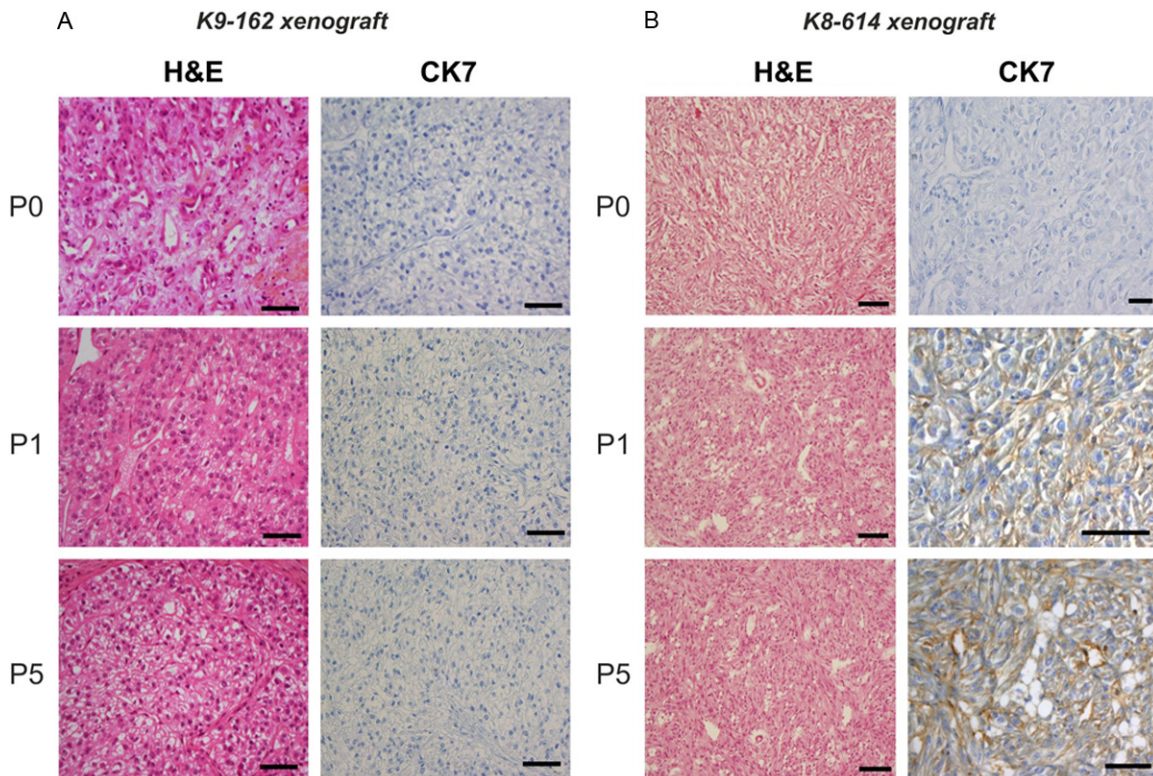


Figure 2. Morphological characterisation at P0 and subsequent passages. Histological features and CK7 immuno-histochemistry for two RCC at P0, P1 and P5: no change was observed for CK7 expression for K9-162 xenograft (A); CK7 was negative at P0 and became positive at P1 for K8-164 xenograft (B); Scale bar = 50 μ m.

tumors reached a volume of 400 to 600 mm³, five mice received 20 mg/kg/day sunitinib diluted in 0.9% NaCl by gavage for 35 days. Five other mice were untreated and used as controls. Tumor growth was followed by measuring tumor volume for 35 days using ultrasound imaging (AplioXT, Toshiba, France). Results were expressed as mean \pm standard error of the mean (SEM).

Phenotype analyses

The initial surgical sample and xenograft samples were fixed in AFA (alcohol-formalin-acetic acid) for three hours and embedded in paraffin. 2 μ m thick sections were stained with hematoxylin and eosin (H&E). Histopathological features of patient tumor tissues were compared with those in the corresponding xenografts on H&E sections.

Immunohistochemical (IHC) studies were carried out with the following primary antibodies: CK7 monoclonal mouse anti-human antibody (DakoCytomation, France, clone OV-TL 12/30) at 1:20 dilution; CD10 monoclonal mouse anti-

human antibody (DakoCytomation, France, clone 56C6) at 1:20 dilution; vimentin monoclonal mouse anti-human antibody (DakoCytomation, France, clone V9) at 1:100 dilution; p53 monoclonal mouse anti-human antibody (Dakocytomation, France, clone DO-7) at 1:50 dilution; CD31 monoclonal rat anti-mouse antibody (Dianova, Germany, clone SZ31) at 1:20 dilution. All the immunostainings were performed in an automated immunostainer (Ventana Medical System, France).

Location of staining and percentage of stained cells were noted by two pathologists (PB, JV). Mitotic counts were determined on 10 microscopic high-power fields (x400).

Results for mitotic counts and vessels counts were expressed as mean \pm standard error of the mean (SEM).

Genomic analyses

Tumor cells were obtained from tissue sections using microdissection (Palm, Germany).

Table 3. Microsatellite analysis on initial tumors (P0) and xenografted tumors at 1st (P1) and 5th (P5) passage in mice

tumor ID	passage	D3S1289	D3S1597	D3S3611	D5S2095	D6S440	D8S1820	D9S162	D9S171	D17S802	D17S1879
K6-194	P0	▲	▲▲	▲▲	▲▲	NA	▲▲	NA	NA	NA	▲
	P1	▲	▲▲	▲▲	▲▲	NA	☒	▲▲	NA	▲▲	▲
	P5	▲	▲▲	▲▲	▲▲	NA	☒	▲▲	NA	▲▲	▲
K8-128	P0	▲	▲▲	▲	▲▲	▲	▲▲	NA	▲	▲▲	▲▲
	P1	▲	NA	▲	▲▲	▲	▲▲	NA	▲	▲▲	▲▲
	P5	▲	NA	▲	▲▲	▲	▲▲	NA	▲	▲▲	▲▲
K8-447	P0	▲▲	▲▲	▲▲	NA	NA	▲	▲▲	▲▲	▲▲	NA
	P1	☒	▲	▲	NA	NA	▲	▲▲	▲▲	▲▲	NA
	P5	NA	▲	NA	NA	NA	▲	▲▲	☒	NA	NA
K8-614	P0	▲▲	▲▲	▲▲	▲▲	▲	▲▲	▲▲	▲▲	▲▲	NA
	P1	▲▲	▲▲	▲	▲▲	NA	▲	▲▲	▲	▲▲	NA
	P5	▲▲	▲▲	▲	▲▲	NA	▲	▲▲	▲	▲▲	▲▲
K9-162	P0	▲▲	▲▲	▲▲	▲▲	NA	▲	▲▲	▲▲	▲▲	▲▲
	P1	NA	▲	▲▲	▲▲	▲▲	▲	▲	▲	☒	▲▲
	P5	▲	▲	▲▲	▲▲	▲	▲	▲	▲	☒	▲▲
K9-229	P0	▲▲	▲	▲▲	▲▲	▲▲	▲	▲	▲▲	▲▲	▲▲
	P1	▲	▲	▲	☒	▲	▲	▲	▲	▲▲	▲▲
	P5	▲	▲	▲	☒	▲	▲	▲	▲	▲▲	▲▲

▲ one allele; ▲▲ two alleles; ☒ two alleles of different sizes compared to alleles in P0. Non-analysable profiles are noted NA.

DNA purification was performed with Qiagen kit. Two-hundred μ L AL buffer were added to tissue and microdissected tumor cells, homogenized and incubated for 10 minutes at 56°C. Two-hundred μ L 100% ethanol (Sigma, France) were added. The mixture was transferred to a QIAamp column and centrifuged for 1 minute at 8,000 rpm (5.9 rcf). The column was put in a new collection tube, 500 μ L AW1 buffer were added and centrifuged for 1 minute. 500 μ L AW2 buffer were added and the column was centrifuged for 1 minute at 10,000 rpm (9.3 rcf). Elution was performed by adding 25 μ L elution buffer, incubating for 5 minutes at room temperature followed by centrifugation for 1 min. at 10,000 rpm (9.3 rcf).

For allelic profiles analysis, Polymerase Chain Reaction (PCR) was performed using 10 ng DNA for each PCR. Characteristics of the ten microsatellite dinucleotide repeat markers are given in **Table 2**. The PCR mix contained 1U Taq Gold (Applied Biosystems, Foster City, CA, USA), 2.5-4 mM $MgCl_2$, 0.2 mM dNTP, 0.2 μ M labeled forward primers (NEDTM, FAM (6-carboxyfluorescein) or VICTM) and 0.2 μ M non-labelled reverse primers. The PCR final volume was 20 μ L. Thirty-five cycles of PCR were performed. After denaturation, the PCR products were run on ABI PRISM 310 Genetic Analyser [18]. The analysis of the migration data was performed with Genescan 3.1 software (Applied Biosystems). Fluorescent allelic profiles obtained from tumors at P0, P1 and P5 were compared.

All profiles were verified with two different experiments.

Comparative genomic hybridization (CGH) analysis

Genomic DNA was isolated from initial renal tumors and from xenografted samples using DNeasy MiniKit (Qiagen, France) according to the manufacturer's protocol.

CGH labeling and hybridization were performed using high-density 244K arrays from Agilent Technologies, as recommended by the manufacturer. Genomic DNA (1 μ g) from the universal reference sample (Agilent, France) and from each experimental sample was double-digested with Alul and RsaI (Promega, Madison, WI) for 2 hours at 37°C. The digested DNAs were labeled with random primers using Agilent Genomic DNA Labeling Kit Plus (Agilent Technologies) for 2 hours at 37°C, according to the manufacturer's instructions. Tumor DNA and universal reference sample DNAs were labeled with Cy5-dUTP and Cy3-dUTP, respectively. Labeled products were purified with Microcon YM-30 filters (Millipore, Billerica, MA). Tumor DNA and reference DNA (G 147A30 004405 Promega, France) were mixed and hybridized with Human Cot I DNA (Invitrogen) at 65°C for 24 hours. Arrays were scanned with an Agilent DNA Microarray Scanner (G2565BA). Log₂ ratios were determined with Agilent Feature Extraction software (v 9.1.3.1) and the

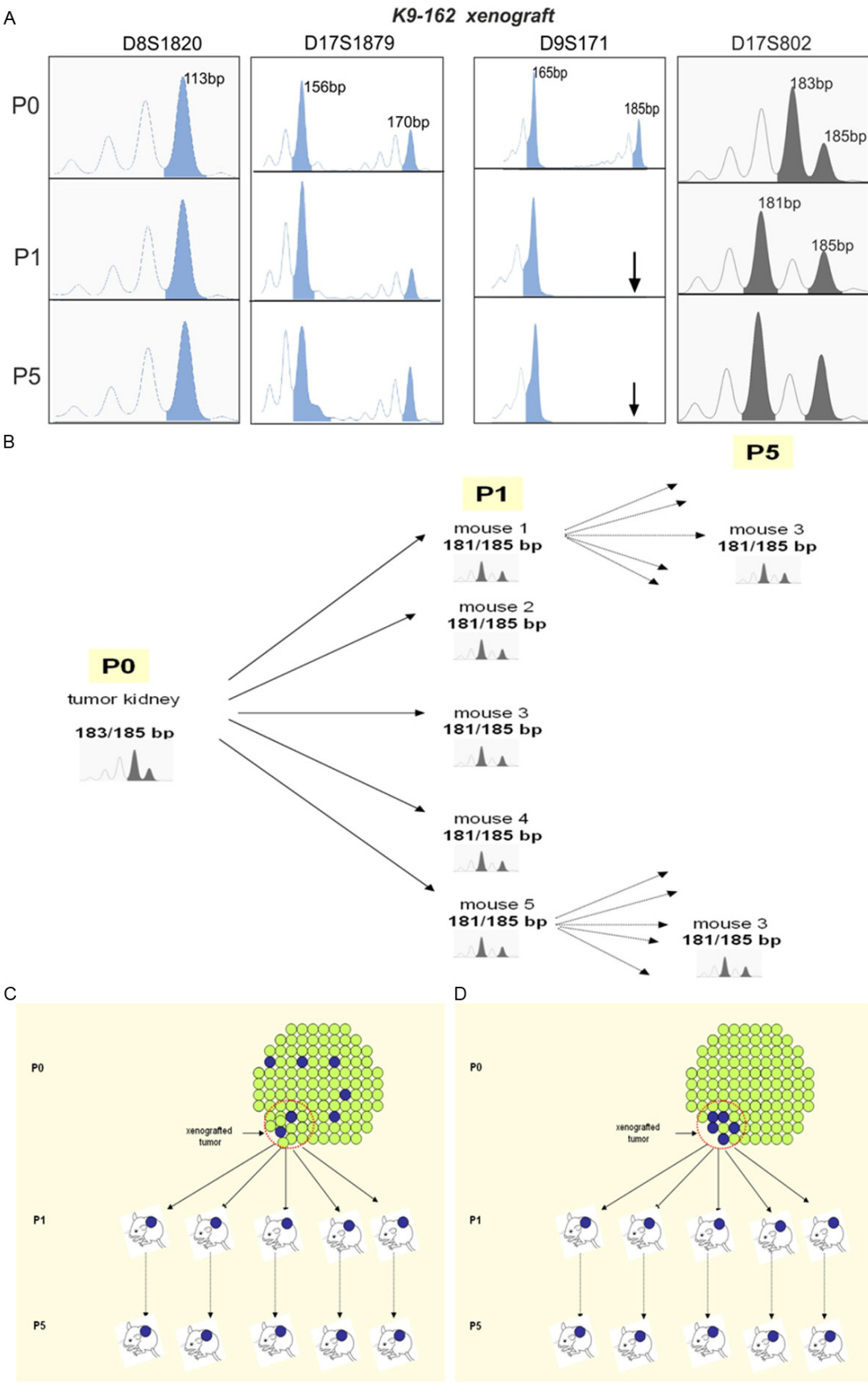


Figure 3. Microsatellite profiles in K9-162 xenograft. (A) Four microsatellite profiles illustrate four situations: The left-hand panels (D8S1820 and D17S1879) show identical profiles from P0 to P5 with one allele (left) or two alleles (center-left). The two right-hand panels (D9S171 and D17S802) show differences from P0 to P5 with different numbers of alleles (center-right) or different size of alleles (right). (B) Distribution of microsatellite profile abnormalities in different mice at the same passage. The new 181 base pair (bp) allele is found in all the mice at the same passage. Cells with abnormalities that were selected at P1 may have been already present at P0 at low levels in the whole tumor (C) or only in the grafted area (D).

global quality of the individual microarrays used in the experiment was validated against the quality metrics (QCmetrics) of this software. Results were analyzed with Agilent's CGH Analytics v3.5 software, and copy number aberrations were detected using the Aberration Detection Method algorithm 2 (ADM-2) using a threshold value of 6.0.

Results

Histopathological characteristics of xenografted human renal tumors

Between 2006 and 2009, 40 kidney tumor samples were subcutaneously grafted into nude mice. Thirty four (85%) primary tumors either developed only as a small tumor less than 3 mm in mice at first passage and could not be further transplanted ($n = 14$ primary tumors), either produced no engraftment at all ($n = 20$ primary tumors). These tumors had a Fuhrman nuclear grade 1, 2 or 3.

Six tumors (15%) showed full xenograft development up to the 5th passage on mice. Clinicopathological data for the six human RCC and the corresponding xenografts in mice at P1 and P5 are given in **Table 1**. The median age of the 6 patients was 64 and all patients already had distant metastases at time of initial diagnosis. One RCC had sarcomatoid cells and one tumor was papillary RCC. The other four RCC contained only clear cells. Fuhrman's nuclear grade was high (3 to 4) for 5 of the 6 RCC. In all six cases, histopathological analysis on H&E sections showed similar morphology of the xenografted tumors and of the corresponding primary tumors, even for the tumor with sarcomatoid changes (K8-614) which showed a double differentiation until the 5th passage.

The preclinical model

We observed in xenografted mice that the speed of tumor growth progressively increased according to the passage: for the development

of a 1500 mm³ graft at P1, it took 5 months on average, compared to 1.5 months at P5 (**Figure 1A**). In all mice we did not observe distant metastasis in sampled organs: lung, liver, spleen, kidney, ovary, bone marrow and brain. There was no significant difference in mitotic index between initial tumors and xenografted tumors at P1 and P5, except for K8-447 which showed an increased number of mitoses at P5 ($P < 0.001$) (**Figure 1B**). Density of blood vessels in xenografted RCC determined using anti mouse CD31, was not statistically different across passages using (**Figure 1C**).

Histopathology stability from P0 to P5

We assessed by IHC the expression of four protein markers, CK7, CD10, vimentin and p53, for all primary primary RCC (**Table 1**). In five out of six cases CK7 expression was unchanged at P5. An example for K9-162 is given in **Figure 2A**. For one case, K8-614 xenograft, the RCC with sarcomatoid cells, showed a strong CK7 expression at P5 (60% positive cells) while P0 was negative (**Figure 2B**).

CD10 and vimentin immunostainings were unchanged from P0 to P5 for all six tumors.

P53 nuclear expression was unchanged in all cases. In only one case (K8-128) a significant cytoplasm staining was found at P5.

Genotypic stability on microsatellite profiles

To determine whether serial xenografts induce changes in genetic profiles, we assessed microsatellite profiles at P0, P1 and P5. Characteristics of the 10 microsatellite markers used in the present study are shown in **Table 2** and were selected because of their frequent deletion in RCC. The microsatellite profiles obtained are shown in **Table 3**. Out of 60 groups of P0-P1-P5 profiles, 44 groups had fully available microsatellite data and could be analyzed. Stability was observed in 66% for all markers. When changes were observed they

Renal cancer xenografts stability

Table 4. CGH analyses in K9-162 at P0 and at P5

chromosome	cytoband	K9-162 P0 ampli /del	K9-162 P5 ampli /del	example of genes in the region
1	p36.33 - p11.2	-0,78	-0,27	GNB1, CALML6, TMEM52
1	p31.2 - p31.1	-1,22	0,74	LRRC7, PIN1L, LRRC40
1	p31.1	-5,56	0,74	NEGR1
1	p21.1	-7,11	-2,76	RWDD3, SLC44A3
1	p13.3	-4,63	-4,48	WDR47
1	q21.1 - q23.1	0,37	-0,17	LOC388692, FCGR1C, FLJ39739, PPIAL4A, NBPFL4
1	q21.3	-0,2	-1,16	TCHHL1, TCHH, RPTN, LCE3C, LCE3B
2	p11.2	-1,089	-0,54	TMSB10, KCMF1, TCF7L1
2	q32.3 - q33.1	-1,03	-0,23	SLC39A10, SLC39A10, DNAH7
2	q33.1 - q37.3	-0,83	-0,25	PFTK2, FZD7, SUMO1
3	p26.3 - p11.1	-0,92	-0,24	CHL1, CNTN6, CNTN4
3	p26.3	-0,92	-0,56	CHL1, CNTN6
3	p11.1	-6,23	-1,9	EPHA3, EPHA3
3	q22.1	-0,35	1,56	COL29A1, COL6A6, PIK3R4, CPNE4
3	q26.1	1,33	0,88	PPM1L
4	p16.3 - q11	-0,96	-0,25	ZNF718, ZNF732, LOC654254
5	q11.2	0,63	-0,53	SLC38A9, DDX4, DDX4
6	p25.3-q11.1	-0,69	-0,25	DUSP22, IRF4, EXOC2
7	p22.3	4,37	-0,4	FAM20C, PDGFA, PRKAR1B
7	q11.21 - q36.3	0,54	0,2	ZNF735, ZNF679, ZNF680
7	q11.22	-0,5	-0,08	AUTS2, AUTS2, AUTS2
7	q31.1	-6,54	-3,61	
7	q34	-4,14	-3,71	ATP6V0A4, KIAA1549, KLRG2, ADCK2
8	p23.3 - q11.1	-0,92	-0,25	ZNF596, FBXO25, RPL23AP53,
8	p23.3 - q11.1	-1,31	-0,25	DLGAP2, CLN8, ARHGEF10
8	q11.1 - q11.23	-1,14	-0,22	KIAA0146, CEBPD, PRKDC
8	q24.3	0,55	-0,33	GML, CYP11B1, CYP11B2, NCRNA00051, TSNARE1, BAI1
9	p24.3 - p13.1	-0,93	-0,25	C9orf66, DOCK8, KANK1,
9	q12 - q34.3	-0,79	-0,27	MGC21881, AQP7P1, AQP7P2
10	p15.3 - p11.21	0,6	0,18	ZMYND11, ZMYND11, DIP2C,
10	q11.23	-4,79	-2,94	PARG, ARHGAP22
10	q26.2 - q26.3	-1,19	-0,63	DOCK1, C10orf141, NPS, BNIP3, JAKMIP3, DPYSL4
10	p15.5 - p15.4	0,44	-0,38	IFITM5, IFITM2, IFITM1, RIC8A, SIRT3, PSMD13
11	q11	3,69	-0,61	OR4P4, OR4S2, OR4C6
11	q12.2 - q14.1	0,4	-0,1	MS4A15, MS4A10, CCDC86, VPS37C, PGA3, PGA4
14	q11.1 - q32.33	-0,82	-0,28	P704P, OR4Q3, OR4M1
15	q11.2	-0,64	-0,73	LOC727832, GOLGA8C,
15	q22.31	-1,21	-0,73	MAP2K1, TIPIN
16	p13.3 - p13.2	-0,19	-0,31	A2BP1, A2BP1, A2BP1, SNRNP25, RHBDF1, MPG
16	q23.1	-0,05	-1,64	WVVOX
17	p13.3 - p13.1	0,5	-0,2	VPS53, VPS53, FAM57A, RPH3AL, C17orf97, FAM101B
17	q11.2	1,37	0,13	PROCA1, RAB34, RAB34
17	q21.33 - q22	-0,11	0,03	MBTD1, UTP18, CA10
18	q23	-4,23	-4,68	MBP, GALR1, SALL3, TXNL4A
19	p13.3	0,74	-0,58	SHC2, ODF3L2, MADCAM1
20	p13	1,34	-0,55	SPEF1, CENPB, CDC25B,
21	q21.1	-4,15	-5,12	TMPRSS15
22	q11.1	-1,06	-0,75	POTEH, OR11H1, CCT8L2
22	q12.3	-1,9	-2,38	RBM9, LARGE
22	q13.33	-1,28	-0,8	ZBED4, ALG12, CRELD2

were of two types: allelic number changes (in 11/44 groups, 25%) or allelic size changes (in

4/44 groups, 9%) (**Figure 3A**). When present in a tumor in one mouse, changes were also pres-

Table 5. CGH analyses in K8-614 at P0 and at P5

chromosome	cytoband	K8-614 P0 ampl /del	K8-614 P5 ampl /del	example of genes in the region
1	p36.23	1,13	4,01	PER3, VAMP3
1	p31.1	1,67	3,34	NEGR1, TNNI3K, CRYZ , PIGK
1	q24.2	-3,5	-2,88	NME7, NME7
2	p16.1	-3,64	-5,66	SMEC2
2	p13.1	-3,79	4,59	SLC4A5, SLC4A5, DQX1
3	p21.31	-4,69	-2,88	SCAP
3	q26.1	-3,86	-3,57	PPM1L, CT64
4	q13.1	-2,28	-5,44	CCRN4L
4	q28.3	-5,394	-5,55	PCDH10
4	q34.1	-3,28	-5,55	GALNTL6
6	p22.3	-3,87	-3,14	RNF144B
6	q12	-3,87	-5,2	EYS
7	q21.11	-3,87	-3,18	SEMA3D
7	q22.1	-6,05	-2,35	ZAN
7	q34	-3,68	-3,7	ATP6V0A4, KIAA1549 , KLRG2, ADCK2
9	p11.2	-2,87	-3,44	UBE2R2, DCAF12
10	q21.3	-2,5	-2,5	DNAJC12
14	q32.33	-2,87	1,35	PPP1R13B, ZFYVE21 , MIR203 ,
18	q23	-3,81	-5,69	MBP , GALR1 , SALL3 , TXNL4A

ent in all other xenografted mice for the same passage (**Figure 3B**). All changes occurred as early as P1 and remained until P5 except for two allelic losses on microsatellites D9S171 (xenograft K8-447) and D6S440 (xenograft K9-162) that appeared only at P5 (**Table 3**). Most changes occurred between P0 and P1 and not after P1. This implies that these aggressive tumor xenografts are intrinsically stable and that changes observed at P1 are likely due to intra-tumor heterogeneity of primary tumors (**Figure 3C**) or only represent a local subclone present in the grafted sample (**Figure 3D**).

Genotypic stability on CGH-arrays

We performed comparative genomic hybridization at P0 and P5 for two RCC (K9-162, K8-614) with enough tissue material available (surgery) at P0. Overall stability of the xenografted tumor genome was observed. Genetic abnormalities detected in initial RCC (P0) were also detected in the corresponding xenografts at P5. Sometimes new deletions or amplifications were detected at P5. Some examples are given in **Tables 4** and **5**.

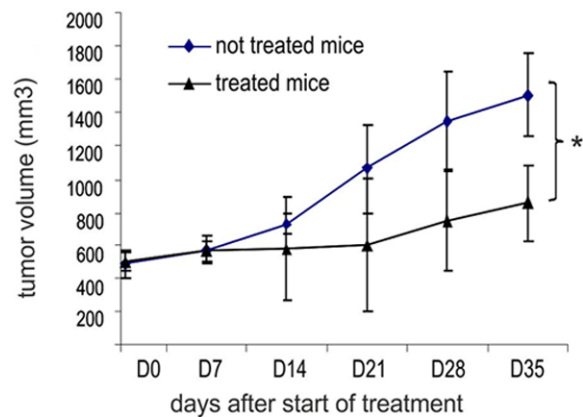
Comparison of response to sunitinib in patients and xenografted human tumors

Follow up data of patients under sunitinib treatment was available for three patients with RCC. Two patients showed a lack of response and one patient showed stable disease after 3 months of treatment with sunitinib followed by secondary resistance. When we studied the response to sunitinib in the three corresponding xenografted RCC, we found similar patterns of response (**Figure 4**).

Discussion

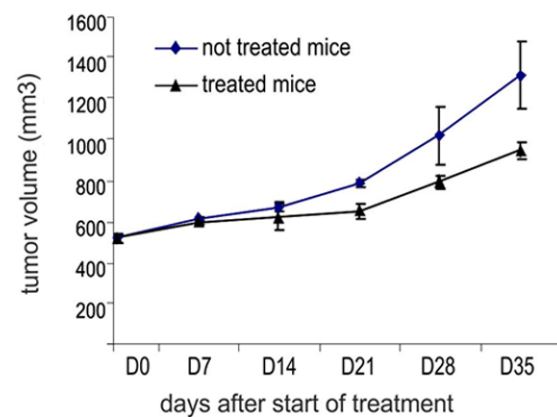
RCC remains a cancer with poor prognosis and short median survival due to frequent metastatic progression [19]. Xenografting human RCC into nude mice offers the opportunity to test new therapies and even personalized therapy [20]. We explored this stability on six xenografted RCC that showed “full engraftment” not only at P1 but also in further passages. In the 14 cases with a small tumor that developed only at P1, the tumor cells were often surrounded by numerous murine lymphocytes. These “incomplete engraftment” cases were mostly

K6-194 xenograft



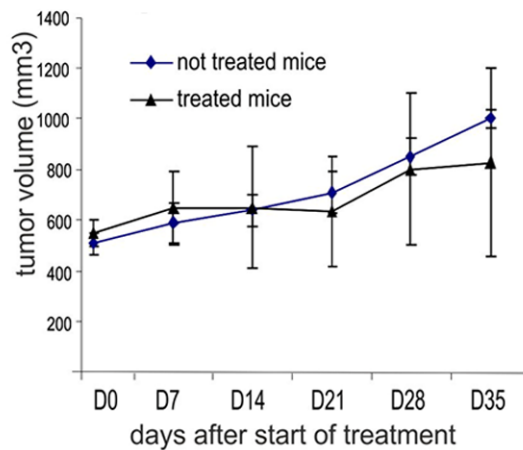
patient data : initial stability followed by secondary progression

K8-614 xenograft



patient data : no response

K9-162 xenograft



patient data : no response

Figure 4. Tumor response profile for sunitinib treatment on three xenografted kidney tumors. A good correlation between tumor xenograft and patient data was observed; * $P < 0.005$.

early stages tumors in patients, therefore probably less aggressive tumors.

All tumors were xenografted subcutaneously in the brown fat. There is no consensus regarding the best site (under the renal capsula or under the skin) to obtain the best RCC engraftment [21, 22]. The time required for engraftment at P1 was longer than the time required for engraftment at the following passages. This was not linked to the volume of grafted RCC or to the proliferative index, or to the microvessel density. A similar discrepancy between the time necessary for the engraftment at P1 and at P5 was reported in human pancreatic cancer xenografts [23]. This could be linked to the new murine environment at P1 or to the initiation of

new blood vessels in the xenografted human cancers. A high degree of similarity between xenografts and initial cancers in terms of histopathology, immunohistochemistry, as well as mutation status, has been reported for non-small cell lung cancer [24-26], gynecological tumors [27], uveal melanoma [28], gastro-esophageal junction cancer [8] and breast cancers [11]. In our series, all six RCC xenografts reproduced the histopathological aspects of the primary RCC including the cases with papillary patterns or sarcomatoid cells. Approximately 8% of ccRCC have components with sarcomatoid changes. Sarcomatoid cells are thought to arise from clear-cell tumors with an accumulation of genetic alterations [29, 30] and have been associated with poor prognosis

[31]. The xenograft model K8-614 with sarcomatoid changes showed histopathological stability until the 5th passage. The overall rates of clear cells and sarcomatoid areas were similar between P0 and P5, therefore making this xenograft a good model of this RCC type.

We observed some differences for CK7 in K8-614 xenograft and for p53 in K8-128 xenograft. This may account for possible cytokeratine microfilaments accumulation and for possible modifications of p53 nuclear export process after several passages in mice. This was concordant with other studies in the literature where some minor changes in immunohistochemical patterns have been observed [28].

Regarding genomic stability, we observed an overall good preservation of the allelic profiles between P0, P1 and P5 (66% identical allelic profiles). Changes were observed in 34% of allelic profiles and were most often present in all mice at the same passage, both in P1 and P5. Two changes were observed only in P5 and were not present in P1. Recently, using SNP-arrays or gene expression analyses, it has been showed very close genotypes between primary renal tumors and xenografted tumors [22, 32, 33]. Our study not only included xenografts at first passage but also at fifth passage, showing that most changes occurred between P0 and P1 and not after P1. This implies that these aggressive tumor xenografts are intrinsically stable and changes observed at P1 are likely due to intra-tumor heterogeneity of primary tumors [34, 35] or represent a local subclone present in the grafted sample [9]. CGH-array was performed on two xenografts at P5 (K9-162, K8-614) and on the initial tumors. On CGH profiles we found only minor genetic differences between P0 and P5.

The fact that tumor grafts in mice can maintain the genomic and gene expression characteristics of the original tumors has been demonstrated in breast cancer [13, 14] and in ovarian and uterine cancers [27]. Another study comparing the genomic characteristics of several tumor types and their derived xenografts, however not including RCC, showed similar genomic profiles [36].

We also evaluated the response to sunitinib in three tumor xenografts (K6-194, K8-614, K9-162) since these three patients were treat-

ed with this drug. We obtained similar response profiles between xenografts and corresponding initial tumors, confirming the value of sub-cutaneous xenograft models in predicting response to chemotherapeutic agents [24].

In conclusion, these aggressive human renal tumors xenografted into mice showed a good phenotypic and genotypic stability with only minor differences occurring mostly between P0 and P1 and likely due to intra-tumor heterogeneity of primary tumors. Moreover, the xenografts treated with sunitinib showed treatment response profiles close to those of the initial tumors. These animal models obtained from human renal tumor samples could therefore be optimal for selection of initial therapy in these poor-prognosis tumors, and could also help in the development of new targeted treatments.

Acknowledgements

This study was supported by grants from Agence Nationale pour la Recherche (ANR-08-EBIO-022-22), ARC (CR/08/7968) Ibisa (RINR 1-2-3), Institut National du Cancer (INCa) and Tumorotheque of Saint Louis Hospital (Paris, France). We thank Ms. Angela Swaine for revision of the English language.

Disclosure of conflict of interest

None.

Address correspondence to: Dr. Philippe Bertheau, AP-HP-Hôpital Saint-Louis, Laboratoire de Pathologie, 1 avenue Claude Vellefaux, Paris, F-75010, France. Tel: +33 1 42 49 41 35; Fax: +33 1 42 49 49 22; E-mail: philippe.bertheau@sls.aphp.fr

References

- [1] Hudes G, Carducci M, Tomczak P, Dutcher J, Figlin R, Kapoor A, Staroslawska E, Sosman J, McDermott D, Bodrogi I, Kovacevic Z, Lesovoy V, Schmidt-Wolf IG, Barbarash O, Gokmen E, O'Toole T, Lustgarten S, Moore L and Motzer RJ. Temsirolimus, interferon alfa, or both for advanced renal-cell carcinoma. *N Engl J Med* 2007; 356: 2271-2281.
- [2] Motzer RJ, Escudier B, Oudard S, Hutson TE, Porta C, Bracarda S, Grunwald V, Thompson JA, Figlin RA, Hollaender N, Urbanowitz G, Berg WJ, Kay A, Lebwohl D and Ravaud A. Efficacy of everolimus in advanced renal cell carcinoma: a double-blind, randomised, placebo-controlled phase III trial. *Lancet* 2008; 372: 449-456.

- [3] Motzer RJ, Hutson TE, Tomczak P, Michaelson MD, Bukowski RM, Rixe O, Oudard S, Negrier S, Szczylik C, Kim ST, Chen I, Bycott PW, Baum CM and Figlin RA. Sunitinib versus interferon alfa in metastatic renal-cell carcinoma. *N Engl J Med* 2007; 356: 115-124.
- [4] Escudier B, Pluzanska A, Koralewski P, Ravaud A, Bracarda S, Szczylik C, Chevreau C, Filipek M, Melichar B, Bajetta E, Gorbunova V, Bay JO, Bodrogi I, Jagiello-Gruszfeld A and Moore N. Bevacizumab plus interferon alfa-2a for treatment of metastatic renal cell carcinoma: a randomised, double-blind phase III trial. *Lancet* 2007; 370: 2103-2111.
- [5] Rini BI, Halabi S, Rosenberg JE, Stadler WM, Vaena DA, Ou SS, Archer L, Atkins JN, Picus J, Czaykowski P, Dutcher J and Small EJ. Bevacizumab plus interferon alfa compared with interferon alfa monotherapy in patients with metastatic renal cell carcinoma: CALGB 90206. *J Clin Oncol* 2008; 26: 5422-5428.
- [6] Talmadge JE, Singh RK, Fidler IJ and Raz A. Murine models to evaluate novel and conventional therapeutic strategies for cancer. *Am J Pathol* 2007; 170: 793-804.
- [7] Sharpless NE and Depinho RA. The mighty mouse: genetically engineered mouse models in cancer drug development. *Nat Rev Drug Discov* 2006; 5: 741-754.
- [8] Dodbiba L, Teichman J, Fleet A, Thai H, Sun B, Panchal D, Patel D, Tse A, Chen Z, Faluyi OO, Renouf DJ, Girgis H, Bandarchi B, Schwock J, Xu W, Bristow RG, Tsao MS, Darling GE, Ailles LE, El-Zimaity H and Liu G. Primary esophageal and gastro-esophageal junction cancer xenograft models: clinicopathological features and engraftment. *Lab Invest* 2013; 93: 397-407.
- [9] Williams SA, Anderson WC, Santaguida MT and Dylla SJ. Patient-derived xenografts, the cancer stem cell paradigm, and cancer pathobiology in the 21st century. *Lab Invest* 2013; 93: 970-982.
- [10] Cespedes MV, Casanova I, Parreno M and Mangues R. Mouse models in oncogenesis and cancer therapy. *Clin Transl Oncol* 2006; 8: 318-329.
- [11] Zhang X, Claerhout S, Prat A, Dobrolecki LE, Petrovic I, Lai Q, Landis MD, Wiechmann L, Schiff R, Giuliano M, Wong H, Fuqua SW, Contreras A, Gutierrez C, Huang J, Mao S, Pavlick AC, Froehlich AM, Wu MF, Tsimelzon A, Hilsenbeck SG, Chen ES, Zuloaga P, Shaw CA, Rimawi MF, Perou CM, Mills GB, Chang JC and Lewis MT. A renewable tissue resource of phenotypically stable, biologically and ethnically diverse, patient-derived human breast cancer xenograft models. *Cancer Res* 2013; 73: 4885-4897.
- [12] Fiebig HH, Maier A and Burger AM. Clonogenic assay with established human tumour xenografts: correlation of in vitro to in vivo activity as a basis for anticancer drug discovery. *Eur J Cancer* 2004; 40: 802-820.
- [13] Marangoni E, Vincent-Salomon A, Auger N, De-georges A, Assayag F, de Cremoux P, de Plater L, Guyader C, De Pinieux G, Judde JG, Rebucci M, Tran-Perennou C, Sastre-Garau X, Sigal-Zafarani B, Delattre O, Dieras V and Poupon MF. A new model of patient tumor-derived breast cancer xenografts for preclinical assays. *Clin Cancer Res* 2007; 13: 3989-3998.
- [14] DeRose YS, Wang G, Lin YC, Bernard PS, Buys SS, Ebbert MT, Factor R, Matsen C, Milash BA, Nelson E, Neumayer L, Randall RL, Stijleman IJ, Welm BE and Welm AL. Tumor grafts derived from women with breast cancer authentically reflect tumor pathology, growth, metastasis and disease outcomes. *Nat Med* 2011; 17: 1514-1520.
- [15] Sausville EA and Burger AM. Contributions of human tumor xenografts to anticancer drug development. *Cancer Res* 2006; 66: 3351-3354; discussion 3354.
- [16] Eisenhauer EA, Therasse P, Bogaerts J, Schwartz LH, Sargent D, Ford R, Dancey J, Arbuck S, Gwyther S, Mooney M, Rubinstein L, Shankar L, Dodd L, Kaplan R, Lacombe D and Verweij J. New response evaluation criteria in solid tumours: revised RECIST guideline (version 1.1). *Eur J Cancer* 2009; 45: 228-247.
- [17] Varna M, Lehmann-Che J, Turpin E, Marangoni E, El-Bouchtaoui M, Jeanne M, Grigoriu C, Ratajczak P, Leboeuf C, Plassa LF, Ferreira I, Poupon MF, Janin A, de Thé H and Bertheau P. p53 dependent cell-cycle arrest triggered by chemotherapy in xenografted breast tumors. *Int J Cancer* 2009; 124: 991-997.
- [18] Varna M, Soliman H, Feugeas JP, Turpin E, Chapelin D, Legres L, Plassa LF, de Roquancourt A, Espie M, Misset JL, Janin A, de Thé H and Bertheau P. Changes in allelic imbalances in locally advanced breast cancers after chemotherapy. *Br J Cancer* 2007; 97: 1157-1164.
- [19] Bukowski RM, Negrier S and Elson P. Prognostic factors in patients with advanced renal cell carcinoma: development of an international kidney cancer working group. *Clin Cancer Res* 2004; 10: 6310S-6314S.
- [20] Bousquet G, Feugeas JP, Ferreira I, Vercellino L, Jourdan N, Bertheau P, de Bazelaire C, Barranger E and Janin A. Individual xenograft as a personalized therapeutic resort for women with metastatic triple-negative breast carcinoma. *Breast Cancer Res* 2014; 16: 401.
- [21] Angevin E, Glukhova L, Pavon C, Chassevent A, Terrier-Lacombe MJ, Goguel AF, Bougaran J, Ardouin P, Court BH, Perrin JL, Vallancien G, Triebel F and Escudier B. Human renal cell carcinoma xenografts in SCID mice: tumorigenicity

- ty correlates with a poor clinical prognosis. *Lab Invest* 1999; 79: 879-888.
- [22] Grisanzio C, Seeley A, Chang M, Collins M, Di Napoli A, Cheng SC, Percy A, Beroukheim R and Signoretti S. Orthotopic xenografts of RCC retain histological, immunophenotypic and genetic features of tumours in patients. *J Pathol* 2011; 225: 212-221.
- [23] Kim MP, Evans DB, Wang H, Abbruzzese JL, Fleming JB and Gallick GE. Generation of orthotopic and heterotopic human pancreatic cancer xenografts in immunodeficient mice. *Nat Protoc* 2009; 4: 1670-1680.
- [24] Cutz JC, Guan J, Bayani J, Yoshimoto M, Xue H, Sutcliffe M, English J, Flint J, LeRiche J, Yee J, Squire JA, Gout PW, Lam S and Wang YZ. Establishment in severe combined immunodeficiency mice of subrenal capsule xenografts and transplantable tumor lines from a variety of primary human lung cancers: potential models for studying tumor progression-related changes. *Clin Cancer Res* 2006; 12: 4043-4054.
- [25] Fichtner I, Rolff J, Soong R, Hoffmann J, Hammer S, Sommer A, Becker M and Merk J. Establishment of patient-derived non-small cell lung cancer xenografts as models for the identification of predictive biomarkers. *Clin Cancer Res* 2008; 14: 6456-6468.
- [26] Dong X, Guan J, English JC, Flint J, Yee J, Evans K, Murray N, Macaulay C, Ng RT, Gout PW, Lam WL, Laskin J, Ling V, Lam S and Wang Y. Patient-derived first generation xenografts of non-small cell lung cancers: promising tools for predicting drug responses for personalized chemotherapy. *Clin Cancer Res* 2010; 16: 1442-1451.
- [27] Press JZ, Kenyon JA, Xue H, Miller MA, De Luca A, Miller DM, Huntsman DG, Gilks CB, McAlpine JN and Wang YZ. Xenografts of primary human gynecological tumors grown under the renal capsule of NOD/SCID mice show genetic stability during serial transplantation and respond to cytotoxic chemotherapy. *Gynecol Oncol* 2008; 110: 256-264.
- [28] Nemati F, Sastre-Garau X, Laurent C, Couturier J, Mariani P, Desjardins L, Piperno-Neumann S, Lantz O, Asselain B, Plancher C, Robert D, Peguillet I, Donnadiou MH, Dahmani A, Bessard MA, Gentien D, Reyes C, Saule S, Barillot E, Roman-Roman S and Decaudin D. Establishment and characterization of a panel of human uveal melanoma xenografts derived from primary and/or metastatic tumors. *Clin Cancer Res* 2010; 16: 2352-2362.
- [29] Jones TD, Eble JN, Wang M, MacLennan GT, Jain S and Cheng L. Clonal divergence and genetic heterogeneity in clear cell renal cell carcinomas with sarcomatoid transformation. *Cancer* 2005; 104: 1195-1203.
- [30] Bostrom AK, Moller C, Nilsson E, Elfving P, Axelsson H and Johansson ME. Sarcomatoid conversion of clear cell renal cell carcinoma in relation to epithelial-to-mesenchymal transition. *Hum Pathol* 2012; 43: 708-719.
- [31] Bullock A, McDermott DF and Atkins MB. Management of metastatic renal cell carcinoma in patients with poor prognosis. *Cancer Manag Res* 2010; 2: 123-132.
- [32] Sivanand S, Pena-Llopis S, Zhao H, Kucejova B, Spence P, Pavia-Jimenez A, Yamasaki T, McBride DJ, Gillen J, Wolff NC, Morlock L, Lotan Y, Raj GV, Sagalowsky A, Margulis V, Cadeddu JA, Ross MT, Bentley DR, Kabbani W, Xie XJ, Kapur P, Williams NS and Brugarolas J. A validated tumorgraft model reveals activity of dovitinib against renal cell carcinoma. *Sci Transl Med* 2012; 4: 137ra175.
- [33] Karam JA, Zhang XY, Tamboli P, Margulis V, Wang H, Abel EJ, Culp SH and Wood CG. Development and characterization of clinically relevant tumor models from patients with renal cell carcinoma. *Eur Urol* 2011; 59: 619-628.
- [34] Shackleton M, Quintana E, Fearon ER and Morrison SJ. Heterogeneity in cancer: cancer stem cells versus clonal evolution. *Cell* 2009; 138: 822-829.
- [35] Gerlinger M, Rowan AJ, Horswell S, Larkin J, Endesfelder D, Gronroos E, Martinez P, Matthews N, Stewart A, Tarpey P, Varela I, Phillimore B, Begum S, McDonald NQ, Butler A, Jones D, Raine K, Latimer C, Santos CR, Nohadani M, Eklund AC, Spencer-Dene B, Clark G, Pickering L, Stamp G, Gore M, Szallasi Z, Downward J, Futreal PA and Swanton C. Intratumor heterogeneity and branched evolution revealed by multiregion sequencing. *N Engl J Med* 2012; 366: 883-892.
- [36] Monsma DJ, Monks NR, Cherba DM, Dylewski D, Eugster E, Jahn H, Srikanth S, Scott SB, Richardson PJ, Everts RE, Ishkin A, Nikolsky Y, Resau JH, Sigler R, Nickoloff BJ and Webb CP. Genomic characterization of explant tumor-graft models derived from fresh patient tumor tissue. *J Transl Med* 2012; 10: 125.